Available online at www.sciencedirect.com
ScienceDirect
Journal of Sound and Vibration 316 (2008) 32–49
JOURNAL OF SOUND AND VIBRATION
www.elsevier.com/locate/jsvi

Structural–acoustic optimization of sandwich cylindrical shells for minimum interior sound transmission

H. Denli[a], J.Q. Sun[b,*]

[a]Department of Mechanical Engineering, University of Delaware, Newark, DE 19716, USA
[b]School of Engineering, University of California, Merced, CA 95344, USA

Received 28 January 2007; received in revised form 16 February 2008; accepted 18 February 2008
Handling Editor: P. Davies
Available online 1 April 2008

Abstract

This paper presents an optimization study of cylindrical sandwich shells to minimize the transmitted sound into the interior induced by the exterior acoustic excitations. The boundary elements and finite elements are, respectively, used to model the interior and exterior acoustics and the vibration of the shell. The design parameters of the optimization are the reinforcement angles of the orthotropic composite materials of the skins and core. The sensitivity analysis of the objective function with respect to the design variables is computed by the adjoint-variable technique. The optimizations of the shell at a single frequency and in a band of frequencies are investigated. From the promising optimization results it is seen that the reinforcement angles in the composite sandwich layers are effective structural design parameters to minimize the sound transmission into the interior without giving up the structural rigidity, particularly at low frequencies where the structural damping is not effective.

1. Introduction

Modern aircraft fuselage design requires better sound and vibration isolation. Optimal design of cylindrical sandwich shells with minimum noise and vibration transmission is a great interest to aerospace industry. Structural–acoustic analysis of cylindrical sandwich shells has been studied in the literature. However, optimization of the shell to minimize the sound transmission into the interior has not been studied thoroughly. This paper presents such an optimization study of cylindrical sandwich shells with anisotropic materials both at a single frequency and over a band of frequencies. The targeted frequencies are below 1 kHz where structural damping is not effective in reducing vibration and sound transmission.

Integrated acoustical and mechanical fuselage designs of cylindrical sandwich shells have been investigated for better sound transmission reduction [1,2]. Thamburaj and Sun have studied vibration and acoustics problems of non-circular cylindrical sandwich shells with the conformal mapping [3]. Optimization of sandwich beams for maximizing sound transmission loss has been conducted with respect to the material

*Corresponding author. Fax: +1 209 228 4047.
E-mail address: jqsun@ucmerced.edu (J.Q. Sun).

0022-460X/$ - see front matter © 2008 Elsevier Ltd. All rights reserved.
doi:10.1016/j.jsv.2008.02.027

parameters that couple the in-plane and out-of-plane deformation [4]. The skin materials and core geometry, comprising honeycomb and truss-like structures, have been considered to reduce sandwich panel vibrations [5]. Optimization of cylindrical isotropic shells has been studied using the weak radiator concept to minimize the radiated sound power [6].

A parallel research to this study has been conducted by Johnson and Cunefare [7]. They have studied the minimization of the sum of the squared acoustic pressure within a cylindrical acoustic cavity due to the vibration of the composite cylinder at a single frequency. The contribution of the current paper lies in the optimization study of cylindrical sandwich shells for minimum sound transmission into the interior both at a single frequency and over a band of frequencies. In this study, the angle of the in-plane fiber reinforcement is considered as a design variable to achieve the minimization.

The paper is organized as follows. In Section 2, the solutions to the exterior acoustic scattering and sound radiation into the shell interior are first obtained with the boundary element method. Section 3 presents the structural response of the cylindrical sandwich shell with the finite element method. In Section 4, we discuss the parametrization of material constants of the sandwich. In particular, we designate the fiber orientation angles of the composite as the design parameters for optimization. The optimization problem is formulated in Section 5. The sensitivity of the structural–acoustic objective function for optimization and the constraint equation on the fundamental frequency with respect to the design parameters is discussion in Section 6. The adjoint variable method for computing sensitivity functions is also introduced. The numerical results are presented in Section 7.

2. Acoustic response with boundary elements

Fig. 1 shows the coordinate system for the exterior and interior acoustic problem of the cylindrical sandwich shell. It is assumed that the shell is closed at both ends with a rigid endcap, and an acoustic baffle covers outside the endcap. The wave equation for the acoustic pressure known as the Helmholtz equation is given by [8]

$$\nabla^2 p(\mathbf{r}) + k^2 p(\mathbf{r}) = -q(\mathbf{r}), \tag{1}$$

where $p(\mathbf{r})$ is the acoustic pressure, $q(\mathbf{r})$ is the acoustic source in the domain, k is the wavenumber ω/c, ω is the frequency and c is the speed of sound. Note that the frequency dependence of the functions $p(\mathbf{r})$ and $q(\mathbf{r})$ is omitted for brevity in this paper. Consider Green's function for the three-dimensional acoustic medium which satisfies the following equation

$$\nabla^2 G(\mathbf{r}|\mathbf{r}_s) + k^2 G(\mathbf{r}|\mathbf{r}_s) = -\delta(\mathbf{r} - \mathbf{r}_s). \tag{2}$$

The solution to the equation and its normal derivative are given by

$$G(\mathbf{r}|\mathbf{r}_s) = \frac{e^{-ikR}}{4\pi R},$$

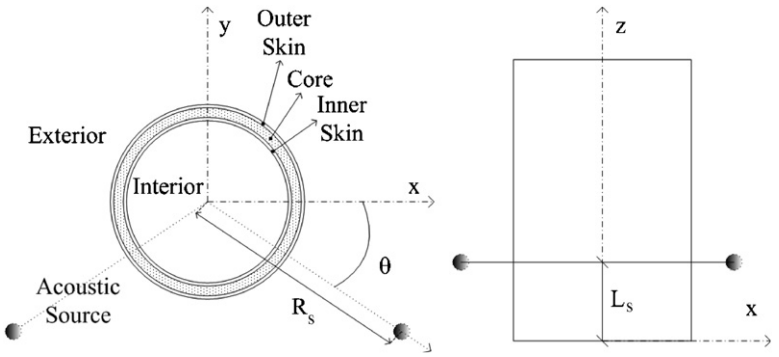

Fig. 1. The coordinate system of the cylindrical shell subject to two point acoustic excitations.

$$\frac{\partial G(\mathbf{r}|\mathbf{r}_s)}{\partial n} = -\left[\frac{\cos\theta}{4\pi R^2} + \frac{\mathrm{i}k\cos\theta}{4\pi R}\right]\mathrm{e}^{-\mathrm{i}kR}, \tag{3}$$

where R is the distance between $\mathbf{r}$ and $\mathbf{r}_s$, θ is the angle between the normal direction n and the vector joining $\mathbf{r}$ and $\mathbf{r}_s$, $\mathbf{r}_s$ denotes the acoustic source location and $\mathbf{r}$ is the observation point.

Combining the Helmholtz equation and Eq. (2), and using the divergence theorems [9], we obtain

$$\int_S \left[p(\mathbf{r}_s)\frac{\partial G(\mathbf{r}|\mathbf{r}_s)}{\partial n_s} - G(\mathbf{r}|\mathbf{r}_s)\frac{\partial p(\mathbf{r}_s)}{\partial n_s}\right] \mathrm{d}S = -Cp(\mathbf{r}) + p_q(\mathbf{r}), \tag{4}$$

where the surface S encloses the acoustic medium in the three-dimensional space V, $\mathbf{r}$ is inside the acoustic medium and n_s is the outward normal of the surface S at $\mathbf{r}_s$. C takes values 1, 1/2 or 0 depending whether the observation point $\mathbf{r}$ is within the acoustic medium, on the surface S or outside the acoustic medium, respectively. $p_q(\mathbf{r})$ is the acoustic sound field generated by the source $q(\mathbf{r})$ in the free three-dimensional space, and is given by

$$p_q(\mathbf{r}) = \int_V G(\mathbf{r}|\mathbf{r}_s)q(\mathbf{r}_s)\,\mathrm{d}V. \tag{5}$$

In the following, we make an assumption that the acoustic energy radiated by the shell is finite such that the acoustic pressure and its gradient vanish as $\mathbf{r} \to \infty$. Green's function $G(\mathbf{r}|\mathbf{r}_s)$ also enjoys these properties as can be seen from Eq. (3). Under this assumption, the surface integration needs only to be computed on the outer boundary of the shell. From now on, S denotes the outer surface of the cylindrical shell.

Let us discretize the surface S into a collection of M boundary elements S_i such that $S = \bigcup_{i=1}^{M} S_i$. Eq. (4) can be rewritten as [10]

$$\sum_{i=1}^{M}\left[\int_{S_i} \frac{\partial G(\mathbf{r}_j|\mathbf{r}_s)}{\partial n_s}\mathbf{N}(\mathbf{r}_s)\,\mathrm{d}S\right]\mathbf{p}_i - \sum_{i=1}^{M}\left[\int_{S_i} G(\mathbf{r}_j|\mathbf{r}_s)\mathbf{N}(\mathbf{r}_s)\,\mathrm{d}S\right]\mathbf{q}_i = -C_j p(\mathbf{r}_j) + p_q(\mathbf{r}_j), \tag{6}$$

where i refers to the source element, j refers to the receiver node, and $\mathbf{N}(\mathbf{r}_s)$ is the shape function. In this work, we use only one type of elements which share the same shape function. The nodal variable vectors $\mathbf{p}_i$ and $\mathbf{q}_i$ of the ith element are defined as

$$\mathbf{p}_i = \begin{Bmatrix} p(\mathbf{r}_{i,1}) \\ p(\mathbf{r}_{i,2}) \\ \vdots \\ p(\mathbf{r}_{i,K}) \end{Bmatrix}, \quad \mathbf{q}_i = \begin{Bmatrix} \dfrac{\partial p(\mathbf{r}_{i,1})}{\partial n_s} \\ \dfrac{\partial p(\mathbf{r}_{i,2})}{\partial n_s} \\ \vdots \\ \dfrac{\partial p(\mathbf{r}_{i,K})}{\partial n_s} \end{Bmatrix}, \tag{7}$$

where $\mathbf{r}_{i,k}$ is the kth node of the ith element and K is the number of nodes of the element. Introducing the following element matrices:

$$\mathbf{B}_{ij} = \int_{S_i} \frac{\partial G(\mathbf{r}_j|\mathbf{r}_s)}{\partial n_s}\mathbf{N}(\mathbf{r}_s)\,\mathrm{d}S,$$

$$\mathbf{E}_{ij} = \int_{S_i} G(\mathbf{r}_j|\mathbf{r}_s)\mathbf{N}(\mathbf{r}_s)\,\mathrm{d}S, \tag{8}$$

we can rewrite Eq. (6) as

$$p_q(\mathbf{r}_j) - C_j p(\mathbf{r}_j) = \sum_{i=1}^{M}\mathbf{B}_{ij}\mathbf{p}_i + \sum_{i=1}^{M}\mathbf{E}_{ij}\mathbf{q}_i. \tag{9}$$

Next, we evaluate $p(\mathbf{r}_j)$ at the nodes of the elements on the surface S.

Let $\mathbf{C}$ denote a diagonal matrix with elements C_j at a proper location, $\mathbf{p}$ be the global vector of the nodal pressure $p(\mathbf{r}_j)$, $\mathbf{q}_i$ be the global vector of the nodal pressure gradient $\partial p(\mathbf{r}_i)/\partial n_s$ along the normal direction n_s, and $\mathbf{p}_q$ be the global vector of the nodal pressure $p_q(\mathbf{r}_j)$. Eq. (9) now reads

$$(\mathbf{C}+\mathbf{B})\mathbf{p}=\mathbf{p}_q-\mathbf{E}\mathbf{q}. \tag{10}$$

2.1. Boundary conditions

When the surface S is rigid without motion, the boundary condition for the acoustic response is given by

$$\mathbf{q}=0. \tag{11}$$

That is, the pressure gradient on the rigid surface vanishes. When the surface is flexible and vibrates, the acoustic boundary condition reads

$$\mathbf{q}=\rho_a\omega^2\mathbf{u}_n, \tag{12}$$

where ρ_a is the mass density of the air, and $\mathbf{u}_n$ is the normal displacement of the surface vibrating at the frequency ω.

Obviously, the above boundary element solution of the acoustic response together with the boundary conditions are general and applicable to both the interior and exterior acoustic problems with respect to the cylindrical shell.

2.2. Remarks

It is well known that Eq. (6) or (10) fails to give a unique solution at certain frequencies which are known as the characteristic frequencies. These frequencies correspond to the natural frequencies of the acoustic medium. One way to avoid this singularity is to add constraints outside the acoustic domain using the combined Helmholtz integral formulation (CHIEF) [10].

3. Vibration of cylindrical sandwich shell

The equations of motion of the cylindrical sandwich shell can be derived by applying Hamilton's principle,

$$\int_{t_1}^{t_2}\delta(T-U+W)\,\mathrm{d}t=0, \tag{13}$$

where T and U are the kinetic and strain energies of the system, and δW is the virtual work done by the external forces. The energies and the virtual work for the sandwich construction can be written as

$$U=\frac{1}{2}\int_D[\sigma_x\varepsilon_x+\sigma_y\varepsilon_y+\sigma_z\varepsilon_z+2\sigma_{xy}\gamma_{xy}+2\sigma_{xz}\gamma_{xz}+2\sigma_{yz}\gamma_{yz}]\,\mathrm{d}V, \tag{14}$$

$$T=\frac{\rho}{2}\int_D[\dot{u}^2+\dot{v}^2+\dot{w}^2]\,\mathrm{d}V, \tag{15}$$

$$\delta W=\int_D\delta\mathbf{u}\cdot\mathbf{f}(\mathbf{r},t)\,\mathrm{d}V+\int_S\delta\mathbf{u}\cdot\mathbf{t}(\mathbf{r},t)\,\mathrm{d}S, \tag{16}$$

where ρ is the mass density, D refers to the physical volume of the shell, S is the surface, (x, y, z) are the global coordinates of the shell, $\mathbf{u}=\{u,v,w\}^{\mathrm{T}}$ is the displacement vector of the shell in (x, y, z) directions, σ_x, σ_y and σ_z are the normal stresses, ε_x, ε_y and ε_z are the normal strains, σ_{xy}, σ_{xz} and σ_{yz} are the shear stresses and γ_{xy}, γ_{xz} and γ_{yz} are the shear strains. $\mathbf{f}(\mathbf{r},t)$ denotes the body force acting on the shell, and $\mathbf{t}(\mathbf{r},t)$ is the surface traction. In this work, we ignore the body force and consider only the normal acoustic pressure acting on the most outer and inner surfaces of the shell as the traction force.

We discretize the shell structure with finite elements. The shape function of the finite element is denoted by **H**. The global coordinates (x, y, z) can be defined as a function of the nodal coordinates by

$$\mathbf{r} = \{x, y, z\} = \mathbf{H}(\mathbf{r})\{\mathbf{x}_e, \mathbf{y}_e, \mathbf{z}_e\}, \tag{17}$$

$$\mathbf{x}_e = \begin{Bmatrix} x_1 \\ x_2 \\ \vdots \\ x_M \end{Bmatrix}, \quad \mathbf{y}_e = \begin{Bmatrix} y_1 \\ y_2 \\ \vdots \\ y_M \end{Bmatrix}, \quad \mathbf{z}_e = \begin{Bmatrix} z_1 \\ z_2 \\ \vdots \\ z_M \end{Bmatrix}, \tag{18}$$

where $(\mathbf{x}_e, \mathbf{y}_e, \mathbf{z}_e)$ denote the vectors of the nodal coordinates, M is the number of the nodes in an element. In the same manner, we obtain the relationship between the global displacements and nodal displacements as

$$\{u, v, w\} = \mathbf{H}(\mathbf{r})\{\mathbf{u}_e, \mathbf{v}_e, \mathbf{w}_e\}, \tag{19}$$

$$\mathbf{u}_e = \begin{Bmatrix} u_1 \\ u_2 \\ \vdots \\ u_M \end{Bmatrix}, \quad \mathbf{v}_e = \begin{Bmatrix} v_1 \\ v_2 \\ \vdots \\ v_M \end{Bmatrix}, \quad \mathbf{w}_e = \begin{Bmatrix} w_1 \\ w_2 \\ \vdots \\ w_M \end{Bmatrix}, \tag{20}$$

where $(\mathbf{u}_e, \mathbf{v}_e, \mathbf{w}_e)$ denote the nodal displacement vectors. Under the assumption of small deformations, the strain–displacement relationship is given by

$$\begin{Bmatrix} \varepsilon_x \\ \varepsilon_y \\ \varepsilon_z \\ \gamma_{xy} \\ \gamma_{xz} \\ \gamma_{yz} \end{Bmatrix} = \begin{bmatrix} \frac{\partial}{\partial x} & 0 & 0 \\ 0 & \frac{\partial}{\partial y} & 0 \\ 0 & 0 & \frac{\partial}{\partial z} \\ \frac{\partial}{\partial y} & \frac{\partial}{\partial x} & 0 \\ \frac{\partial}{\partial z} & 0 & \frac{\partial}{\partial x} \\ 0 & \frac{\partial}{\partial z} & \frac{\partial}{\partial y} \end{bmatrix} \begin{Bmatrix} u \\ v \\ w \end{Bmatrix}. \tag{21}$$

Let **u** denote the assembled vector of all the nodal displacements $(\mathbf{u}_e, \mathbf{v}_e, \mathbf{w}_e)$. The strain can be written as $\boldsymbol{\varepsilon} = \mathbf{B}\mathbf{u}$ for each element where $\boldsymbol{\varepsilon} = \{\varepsilon_x, \varepsilon_y, \varepsilon_z, \gamma_{xy}, \gamma_{xz}, \gamma_{yz}\}^{\mathrm{T}}$ and the matrix **B** contains the derivatives of the shape functions defined through Eq. (21). In this work, we consider anisotropic materials. The constitutive equations of the lth layer are given by

$$\boldsymbol{\sigma} = \mathbf{Q}_l \boldsymbol{\varepsilon}. \tag{22}$$

where $\boldsymbol{\sigma} = \{\sigma_x, \sigma_y, \sigma_z, \sigma_{xy}, \sigma_{xz}, \sigma_{yz}\}^{\mathrm{T}}$ and $\mathbf{Q}_l$ is a 6×6 matrix.

Consider the harmonic problem. In this study, we assume that there are two acoustic volume velocity point sources located at $R_s = 10\,\mathrm{m}$, $L_s = 2\,\mathrm{m}$ and $\theta = \frac{-1}{12}\pi$ and $\theta = \frac{13}{12}\pi$ *rad* outside the cylindrical shell as shown in Fig. 1. The air density is $\rho_a = 1.21\,\mathrm{kg/m^3}$ and the speed of sound is $c = 340.2\,\mathrm{m/s}$. The shell is excited by the acoustic pressure only. The acoustic pressure distribution over an element of the outer or inner surface of the cylindrical shell can be expressed in terms of the nodal pressure values and the shape function,

$$p(\mathbf{r}) = \mathbf{N}(\mathbf{r})\mathbf{p}_e, \tag{23}$$

where $\mathbf{N}(\mathbf{r})$ is the shape function for the surface element and $\mathbf{p}_e$ is the nodal vector of the acoustic pressure on the boundary element defined in Section 2. Note that the outer and inner surfaces of the shell are discrete with

the same boundary elements as for the acoustic problem. We write the variation of the kinetic and strain energies and the virtual work for all the layers as

$$\delta U = \delta \mathbf{u}^H \sum_{e\triangleq 1}^{N} \sum_{l\triangleq 1}^{N_l} \left[\int_{D_e} \mathbf{B}^{\mathrm{T}} \mathbf{Q}_l \mathbf{B} \, \mathrm{d}V \right] \mathbf{u},$$

$$\delta T = \delta \mathbf{u}^H \sum_{e\triangleq 1}^{N} \sum_{l\triangleq 1}^{N_l} \left[\omega^2 \rho_l \int_{D_e} \mathbf{H}^{\mathrm{T}} \mathbf{H} \, \mathrm{d}V \right] \mathbf{u},$$

$$\delta W = \delta \mathbf{u}^H \sum_{e\triangleq 1}^{N} \left[\int_{S_e} \mathbf{N}^{\mathrm{T}} \mathbf{p}_e \, \mathrm{d}S \right], \tag{24}$$

where the symbol $\triangleq$ implies the assembly of element matrices in this paper, $\mathbf{u}$ is the global nodal displacement vector assembled from all the vectors $(\mathbf{u}_e, \mathbf{v}_e, \mathbf{w}_e)$, $\delta\mathbf{u}$ is the corresponding virtual global displacement vector and D_e is an individual element volume. N_l is the number of the layers and $N = N_r \times N_z$ where N_r is the number of elements in the circumferential direction and N_z is the number of elements along the axial direction. Note that the assembly of the sandwich system can be decomposed into in-plane and transverse components. Hamilton's principle together with Eq. (24) leads to the equations of motion as

$$(\hat{\imath} b - \omega^2)\mathbf{M}\mathbf{u} + (\lambda^2 + \hat{\imath} a)\mathbf{K}\mathbf{u} = \mathbf{f}, \tag{25}$$

where $\hat{\imath} = \sqrt{-1}$ and

$$\mathbf{M} = \sum_{e\triangleq 1}^{N} \sum_{l\triangleq 1}^{N_l} \left[\omega^2 \rho_l \int_{V_e} \mathbf{H}^{\mathrm{T}} \mathbf{H} \, \mathrm{d}V \right],$$

$$\mathbf{K} = \sum_{e\triangleq 1}^{N} \sum_{l\triangleq 1}^{N_l} \left[\int_{V_e} \mathbf{B}^{\mathrm{T}} \mathbf{Q}_l \mathbf{B} \, \mathrm{d}V \right],$$

$$\mathbf{f} = \sum_{e\triangleq 1}^{N} \left[\int_{S_e} \mathbf{N}^{\mathrm{T}} \mathbf{p}_e \, \mathrm{d}S \right]. \tag{26}$$

We have assumed a Rayleigh damping as $\mathbf{C} = a\mathbf{K} + b\mathbf{M}$ where a and b are prespecified constants.

3.1. A computational note

The calculation of the global stiffness and mass matrices $\mathbf{K}$ and $\mathbf{M}$ can be simplified for the sandwich element construction shown in Fig. 2. When the cylindrical shell is discretized uniformly in the radial and axial directions as in Fig. 3, and each layer is made of a uniform material, elemental stiffness and mass matrices $\mathbf{K}_e$ and $\mathbf{M}_e$ are required to be calculated *only once* for each layer in the local coordinates. The elemental matrices can then be rotated by an angle φ_i and assembled along the thickness direction. The stiffness and mass matrices $\mathbf{K}$ and $\mathbf{M}$ assembled in this manner can now be denoted as

$$\mathbf{M} = \sum_{j=1}^{N_z} \sum_{i=1}^{N_r} \sum_{l=1}^{N_l} (\mathbf{T}_i^{\mathrm{T}} \mathbf{M}_l \mathbf{T}_i)_j,$$

$$\mathbf{K} = \sum_{j=1}^{N_z} \sum_{i=1}^{N_r} \sum_{l=1}^{N_l} (\mathbf{T}_i^{\mathrm{T}} \mathbf{K}_l \mathbf{T}_i)_j, \tag{27}$$

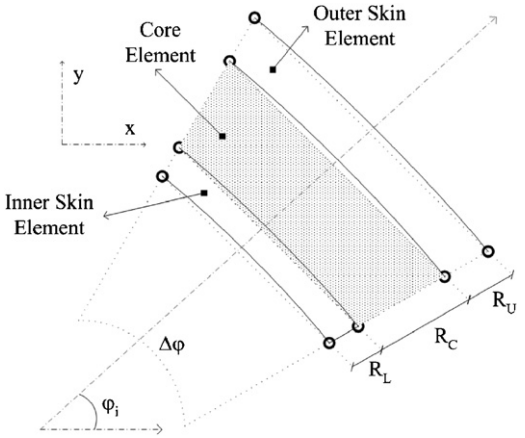

Fig. 2. The structural element of the cylindrical shell.

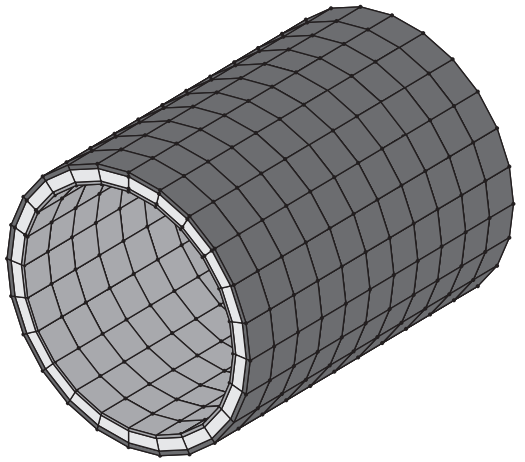

Fig. 3. The structural finite element mesh of the cylindrical sandwich shell.

where $N_l = 3$ in this application, index j refers to the assembly along the axial direction of the shell, the matrices $\mathbf{T}_i^{\mathrm{T}}\mathbf{M}_l\mathbf{T}_i$ and $\mathbf{T}_i^{\mathrm{T}}\mathbf{K}_l\mathbf{T}_i$ are not a function of index j and $\mathbf{T}_i$ is the transformation matrix from the local coordinate to the global coordinate defined as

$$\mathbf{T}_i = \begin{bmatrix} \mathbf{T}_{ii} & & & \\ & \mathbf{T}_{ii} & & \\ & & \ddots & \\ & & & \mathbf{T}_{ii} \end{bmatrix},$$

$$\mathbf{T}_{ii} = \begin{bmatrix} \cos(\varphi_i) & \sin(\varphi_i) & \\ -\sin(\varphi_i) & \cos(\varphi_i) & \\ & & 1 \end{bmatrix}. \tag{28}$$

The dimension of the transformation matrix $\mathbf{T}_i$ is the $3M \times 3M$. Recall that M is the number of nodes in an element.

In Eq. (27), the elemental matrices $\mathbf{M}_l$ and $\mathbf{K}_l$ are required to be computed only N_l times where N_l is the number of layers, and remain the same for different indices i and j. The transformation matrix is required to

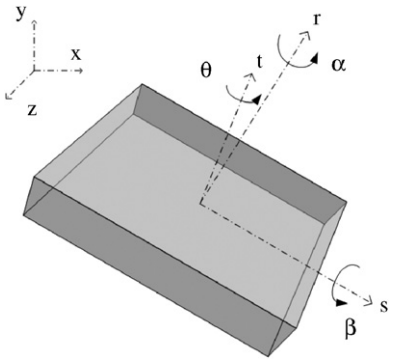

Fig. 4. The reinforcement angles of the composite as design parameters.

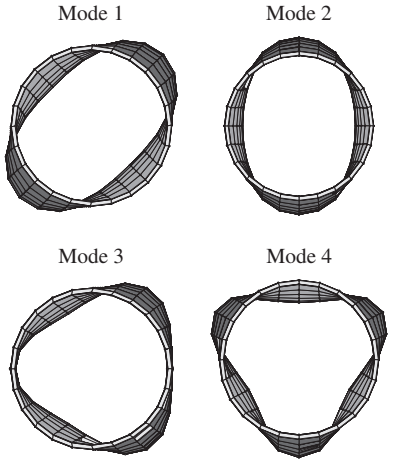

Fig. 5. The first four natural modes of the cylindrical sandwich shell. Their frequencies are 68.70, 70.35, 72.02 and 82.25 Hz.

be computed N_r times where N_r is the number of circumferential elements. Along the axial direction, the same matrices are assembled. This assembly process can save a huge amount of computational time in the construction of the system matrices since the volume integrations in Eq. (26) are numerically computed only N_l times.

The natural frequencies and modes of the cylinder can be obtained from the following eigenvalue problem:

$$[\mathbf{K} - \omega_j^2 \mathbf{M}]\boldsymbol{\phi}_j = 0, \tag{29}$$

where $\boldsymbol{\phi}_i^{\mathrm{T}} \mathbf{M} \boldsymbol{\phi}_j = \delta_{ij}$, ω_j^2 are the eigenvalues and $\boldsymbol{\phi}_j$ are the associated eigenvectors. Examples of the first four mode shapes of the cylindrical shell are exhibited in Fig. 5 and the corresponding natural frequencies are 68.70, 70.35, 72.02 and 82.25 Hz.

4. Material parametrization

The material properties of the layers are parametrized by the angles shown in Fig. 4. Angles α, β and θ indicate reinforcement orientations along the local coordinates r, s (out-of-plane normals) and t (in-plane normal). The reinforcement orientation for the skins and core can be given as

$$\bar{\mathbf{Q}}_l = \mathbf{T}_\theta^{-1} \mathbf{T}_\beta^{-1} \mathbf{T}_\alpha^{-1} \mathbf{Q}_l \mathbf{T}_\alpha \mathbf{T}_\beta \mathbf{T}_\theta, \tag{30}$$

where $\bar{\mathbf{Q}}_l$ refers to the material stiffness matrix after the transformation, $\mathbf{T}_\alpha$, $\mathbf{T}_\beta$ and $\mathbf{T}_\theta$ are the transformation matrices [11,12]. For instance, the in-plane transformation matrix is

$$\mathbf{T}_\theta = \begin{bmatrix} \cos^2\theta & \sin^2\theta & 0 & 0 & 0 & \sin(2\theta) \\ \sin^2\theta & \cos^2\theta & 0 & 0 & 0 & -\sin(2\theta) \\ 0 & 0 & 1 & 0 & 0 & 0 \\ 0 & 0 & 0 & \cos\theta & -\sin\theta & 0 \\ 0 & 0 & 0 & \sin\theta & \cos\theta & 0 \\ -\sin(2\theta)/2 & \sin(2\theta)/2 & 0 & 0 & 0 & \cos^2\theta - \sin^2\theta \end{bmatrix}, \tag{31}$$

and the out-of-plane transformation matrices are similarly structured as a function of α and β.

4.1. Baseline configuration

The optimization study takes a baseline configuration of the sandwich shell as an initial condition. The length and inner radius of the cylinder is 6 and 2 m. The thicknesses of the inner skin, core and outer skin are 0.01, 0.1 and 0.01 m, respectively. The skins of the baseline cylinder are made of S-Glass/Epoxy and are transversely isotropic. The core is made of in-plane symmetric generic material. The material properties are listed in Table 1. Angles α and β determine the out-of plane reinforcement directions for the core; and angle θ determines the in-plane reinforcement direction for the skins. Since the skin materials are transversely symmetric and the core material is in-plane symmetric, the reinforcement orientation for the skins and core are given as

$$\bar{\mathbf{Q}}_s = \mathbf{T}_\theta^{-1}\mathbf{Q}_s\mathbf{T}_\theta,$$

$$\bar{\mathbf{Q}}_c = \mathbf{T}_\beta^{-1}\mathbf{T}_\alpha^{-1}\mathbf{Q}_c\mathbf{T}_\alpha\mathbf{T}_\beta, \tag{32}$$

The orthotropic material stiffness matrices of the skin and core $\mathbf{Q}_s$ and $\mathbf{Q}_c$ can be expressed in terms of the elastic moduli and Poisson ratios as [11]

$$Q_{11} = \frac{(1-\nu_{23}\nu_{32})}{E_2E_3\Delta}, \quad Q_{12} = \frac{(\nu_{12}+\nu_{32}\nu_{13})}{E_1E_3\Delta},$$

$$Q_{13} = \frac{(\nu_{13}+\nu_{12}\nu_{23})}{E_1E_2\Delta}, \quad Q_{22} = \frac{(1-\nu_{13}\nu_{31})}{E_1E_3\Delta},$$

$$Q_{23} = \frac{(\nu_{23}+\nu_{21}\nu_{13})}{E_1E_3\Delta}, \quad Q_{33} = \frac{(1-\nu_{12}\nu_{21})}{E_1E_2\Delta},$$

$$Q_{44} = G_{23}, \quad Q_{55} = G_{31}, \quad Q_{66} = G_{12}, \quad \frac{\nu_{ij}}{E_i} = \frac{\nu_{ji}}{E_j},$$

Table 1
The material constants of the sandwich layers

Material	ρ (kg/m^3)	E_1 (10 MPa)	E_2 (10 MPa)	G_{12} (10 MPa)	ν_{12}
S-Glass/Epoxy	1760	5380	1790	896	0.25
Generic core	130	10.8	10.8	4.12	0.31
Material	E_3 (10 MPa)	G_{13} (10 MPa)	ν_{13}	G_{23} (10 MPa)	ν_{23}
S-Glass/Epoxy	1790	896	0.25	345	0.34
Generic core	2.0	0.6	0.3	0.6	0.3

$$\Delta = \frac{1 - v_{12}v - v_{23}v_{32} - v_{31}v_{13} - 2v_{21}v_{32}v_{13}}{E_1E_2E_3}, \tag{33}$$

where E_i is the elastic modulus along the i direction, G_{ij} is the shear modulus over the $i-j$ plane and v_{ij} is the Poisson ratio between directions i and j.

5. Optimization formulation

The optimization problem seeks for a structure that transmits minimum acoustic power into the interior in the given frequency band when excited by exterior acoustic sources. The structural–acoustic optimization problem is stated as

$$\text{minimize} \quad W_t(\mathbf{b}) = \frac{1}{\omega_2 - \omega_1}\int_{\omega_1}^{\omega_2} W(\omega, \mathbf{b})\,\mathrm{d}\omega, \tag{34}$$

$$\text{subject to} \quad \begin{cases} b_i^l \leqslant b_i \leqslant b_i^u, \\ -\omega_f(\mathbf{b}) + \omega_0 \leqslant 0, \end{cases} \tag{35}$$

where the lower and upper limits of the frequency band are ω_1 and ω_2, $\mathbf{b}$ is a vector of design parameters such as the material reinforcement angles, b_i^l and b_i^u are the lower and upper bounds of the ith design parameter, $\omega_f(\mathbf{b})$ is the fundamental frequency of the shell and ω_0 is the allowable minimum fundamental frequency. Note that the constraint on the fundamental frequency is meant to maintain the static stiffness and structural integrity of the system. This is a common practice in structural optimization studies. Assume that there are m inequality constraints and n equality constraints. The inequality constraints can be converted to equality constraints by introducing m slack variables as follows:

$$c_j(b_1, \ldots, b_n) + b_{j+n}^2 = 0, \quad j = 1, \ldots, m, \tag{36}$$

where $c_j(b_1, \ldots, b_n)$ is a shorthand notation of the constraint function. We expand the design parameter vector to be $\mathbf{b} = [b_1, \ldots b_n, \ldots, b_{n+m}]^{\mathrm{T}}$. Define the Lagrangian function

$$L(\mathbf{b}, \boldsymbol{\lambda}) = W_t(\mathbf{b}) + \boldsymbol{\lambda}^{\mathrm{T}}\mathbf{c}(\mathbf{b}), \tag{37}$$

where $\boldsymbol{\lambda} \in R^{n+m}$ denotes the vector of Lagrange multipliers. The quasi-Newton gradient descent searching algorithm is used to solve the optimization problem. It should be noted that there are many other searching algorithms available in Ref. [13]. A performance comparison of all the algorithms for the present structural–acoustic optimization problem is out of the scope of the paper.

The transmitted acoustic power through the cylindrical shell into its interior is the objective function given by

$$W(\omega, \mathbf{b}) = \int_{S_{in}} \left(\frac{1}{T}\int_0^{\mathrm{T}} p(\mathbf{r})\mathrm{e}^{\mathrm{j}\omega t} v_n^*(\mathbf{r})\mathrm{e}^{-\mathrm{j}\omega t}\,\mathrm{d}t \right) \mathrm{d}S, \tag{38}$$

where $T = 2\pi/\omega$ is the period, $p(\mathbf{r})$ is the acoustic pressure on the interior surface of the shell, $v_n(\mathbf{r})$ is the normal velocity of the inner surface S_{in}. With the discretization of the surface using the same finite elements as discussed earlier, Eq. (38) can be rewritten as a sum of surface integrations over each element,

$$W(\omega, \mathbf{b}) = \sum_{e=1}^{M} \int_{S_{\mathrm{in}}^e} p(\mathbf{r}) v_n^*(\mathbf{r})\,\mathrm{d}S. \tag{39}$$

With the finite element representation of the shell vibration response, we have

$$v_n(\mathbf{r}) = \mathrm{j}\omega\mathbf{N}(\mathbf{r})\mathbf{u}_n^e = \mathrm{j}\omega\mathbf{N}(\mathbf{r})\mathbf{G}_e\mathbf{u} \tag{40}$$

where $\mathbf{G}_e$ is the linear operator that extracts the normal element displacements from the global displacement vector. Substituting Eq. (12) into Eq. (9) when $p_q(\mathbf{r}) = 0$, we obtain

$$p(\mathbf{r}) = \mathbf{N}(\mathbf{r})\mathbf{p}^e = \rho_a\omega^2\mathbf{N}(\mathbf{r})(\mathbf{C} + \mathbf{B})^{-1}\mathbf{E}\mathbf{G}_e\mathbf{u}, \quad \mathbf{r} \in S_{\mathrm{in}}^e.$$

Thus,

$$W(\omega,\mathbf{b}) = (\mathrm{j}\rho_a\omega^3)\mathbf{u}^H\left(\sum_{e\triangleq 1}^{M}\mathbf{G}_e^{\mathrm{T}}\int_{S_{\mathrm{in}}^e}\mathbf{N}^{\mathrm{T}}(\mathbf{r})\mathbf{N}(\mathbf{r})\,\mathrm{d}S(\mathbf{C}+\mathbf{B})^{-1}\mathbf{E}\mathbf{G}_e\right)\mathbf{u}. \tag{41}$$

Expressing W in the matrix form, we obtain

$$W(\omega,\mathbf{b}) = \mathbf{u}^H\mathbf{A}\mathbf{u} = \mathbf{u}^H\mathbf{A}_s\mathbf{u}, \tag{42}$$

where $\mathbf{A}$ is the acoustic coupling matrix defined in Eq. (41)

$$\mathbf{A} = (\mathrm{j}\rho_a\omega^3)\left(\sum_{e\triangleq 1}^{M}\mathbf{G}_e^{\mathrm{T}}\int_{S_{\mathrm{in}}^e}\mathbf{N}^{\mathrm{T}}(r)\mathbf{N}(r)\,\mathrm{d}S(\mathbf{C}+\mathbf{B})^{-1}\mathbf{E}\mathbf{G}_e\right) \tag{43}$$

and $\mathbf{A}_s = \mathbf{A}_s^H$ is the symmetrical part of $\mathbf{A}$.

6. Sensitivity analysis

Sensitivity analyses can help improve the accuracy and efficiency of the optimization process. It is advantageous to obtain analytical expressions for sensitivity functions. The objective function W is a function of the design parameters $\mathbf{u} = \mathbf{u}(b_1, b_2, \ldots, b_n)$ as indicated. Hence, we can compute the partial derivatives of the objective function with respect to the design variables. Consider the objective function defined in Eq. (42). We have

$$\frac{\partial W}{\partial b_i} = \frac{\partial W}{\partial \mathbf{u}}\frac{\partial \mathbf{u}}{\partial b_i} = 2\mathbf{u}^H\mathbf{A}_s\frac{\partial \mathbf{u}}{\partial b_i}. \tag{44}$$

Assume that the external excitation of the system is independent of the design parameters. $\partial\mathbf{u}/\partial b_i$ can be obtained from the direct differentiation of the equation of motion (25). We have,

$$[(\hat{\imath}b-\omega^2)\mathbf{M} + (1+\hat{\imath}a)\mathbf{K}]\frac{\partial \mathbf{u}}{\partial b_i} = -\left[(\hat{\imath}b-\omega^2)\frac{\partial \mathbf{M}}{\partial b_i} + (1+\hat{\imath}a)\frac{\partial \mathbf{K}}{\partial b_i}\right]\mathbf{u}. \tag{45}$$

This sensitivity analysis requires the solution of Eq. (45) for each design parameter. Alternatively, we can apply the method of adjoint variable. Define an adjoint variable $\mathbb{z}$ satisfying the following equation:

$$[(\hat{\imath}b-\omega^2)\mathbf{M} + (1+\hat{\imath}a)\mathbf{K}]\mathbb{z} = \frac{\partial W}{\partial \mathbf{u}} = 2\mathbf{A}_s\mathbf{u}. \tag{46}$$

When the structure is excited at a single frequency, Eq. (46) is in the same form as the equation of motion with $\mathbb{z}$ as the response and the right-hand side term $2\mathbf{A}_s\mathbf{u}$ as the force vector when $\mathbf{u}$ is available. Thus, it can be solved by using the normal modes of the equation of motion (25) [14].

Eqs. (44)–(46) are combined to yield the gradient

$$\frac{\partial W}{\partial b_i} = -\mathbb{z}^{\mathrm{T}}\left[(\hat{\imath}b-\omega^2)\frac{\partial \mathbf{M}}{\partial b_i} + (1+\hat{\imath}a)\frac{\partial \mathbf{K}}{\partial b_i}\right]\mathbf{u}. \tag{47}$$

Note that the partial derivatives $\partial\mathbf{M}/\partial b_i$ and $\partial\mathbf{K}/\partial b_i$ with respect to b_i on the right-hand side of the equation can often be obtained in an analytical form.

Since the fundamental frequency of the structure is used as a constraint in optimization, its sensitivity with respect to the design parameters is also needed. The sensitivities of the natural frequencies with respect to design variables can be obtained by directly differentiating the eigenvalue problem in Eq. (29). We obtain

$$\left[\frac{\partial \mathbf{K}}{\partial b_i} - \omega_j^2\frac{\partial \mathbf{M}}{\partial b_i} - \frac{\partial \omega_j^2}{\partial b_i}\mathbf{M}\right]\boldsymbol{\phi}_j + [\mathbf{K}-\omega_j^2\mathbf{M}]\frac{\partial \boldsymbol{\phi}_j}{\partial b_i} = 0. \tag{48}$$

Premultiplying the above equation by $\boldsymbol{\phi}_j^{\mathrm{T}}$ and recognizing that $\boldsymbol{\phi}_j^{\mathrm{T}}[\mathbf{K}-\omega_j^2\mathbf{M}]=0$, we obtain

$$\frac{\partial\omega_j^2}{\partial b_i}=\boldsymbol{\phi}_j^{\mathrm{T}}\left[\frac{\partial\mathbf{K}}{\partial b_i}-\omega_j^2\frac{\partial\mathbf{M}}{\partial b_i}\right]\boldsymbol{\phi}_j. \tag{49}$$

7. Numerical results

Before presenting the numerical results, we should point out that the finite element model and the computer programs of this work have been verified with analytical or numerical solutions for special cases available in the literature. For the sake of space, we shall not discuss this further.

Recall that the discretizations of the boundaries of the exterior/interior acoustic media and the outer/inner surfaces of the sandwich cylindrical shell share the same nodes because the same elements and shape functions are used for both the acoustic media and the shell structure. A 4-node two-dimensional *linear element* is chosen for the acoustic boundaries and an 8-node three-dimensional linear element type is taken for the layers of the sandwich shell [15]. The boundary of the interior or exterior acoustic media is discretized by 24 uniform elements circumstantially and 11 uniform elements axially, leading to a total of 264 elements.

The acoustic pressure distributions on the outer surface of the shell obtained from Eq. (10) subject to the boundary condition in Eq. (11) and the external acoustic excitations at 100 and 200 Hz are plotted in Fig. 6. The figure shows the total pressure amplitude of the incident and scattering waves. This pressure distribution will be applied as a load to the shell on the outer surface.

When applied to the interior acoustics, Eq. (12) requires the structural displacements normal to the inner surface of the shell. The displacements on the inner surface are obtained from the vibration analysis in Section 3. The solutions of Eq. (10) for the interior boundary condition with $\mathbf{p}_q=0$ and for the coupled structural–acoustic boundary condition are obtained at 100 and 200 Hz. The acoustic pressure on the inner surface of the shell is shown in Fig. 7. Note that for the interior acoustic problem, the reverse fluid loading on the shell structure is neglected in the vibration analysis.

While the outer and inner surfaces of the shell are discretized with the same element as the boundary elements of the acoustic media, along the thickness direction, each layer has only one element. The total number of structural elements is 792. The mesh of the shell is shown in Fig. 3. In the baseline structure, the in-plane reinforcement direction is $\theta=0$ for both the inner and outer skin materials. The out-of-plane reinforcement angles are $\alpha=0$ and $\beta=0$ for the core material. An example of the objective function for the baseline shell is shown in Fig. 8. The objective function W in dB is calculated as

$$W(\mathrm{dB})=10\log_{10}\left(\frac{W}{W_{\mathrm{ref}}}\right), \tag{50}$$

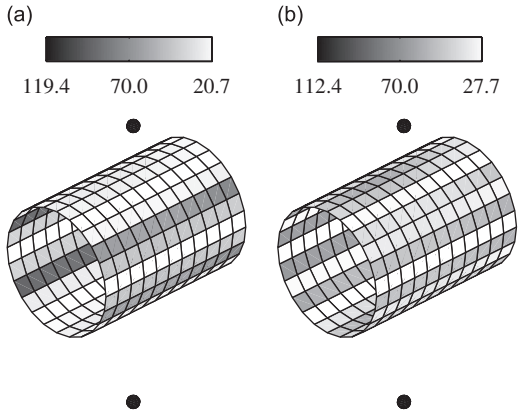

Fig. 6. The acoustic pressure amplitude on the outer surface of the cylindrical shell due to the external acoustic point excitations at (a) 100 and (b) 200 Hz. The shell is treated as a rigid body in the exterior acoustic analysis.

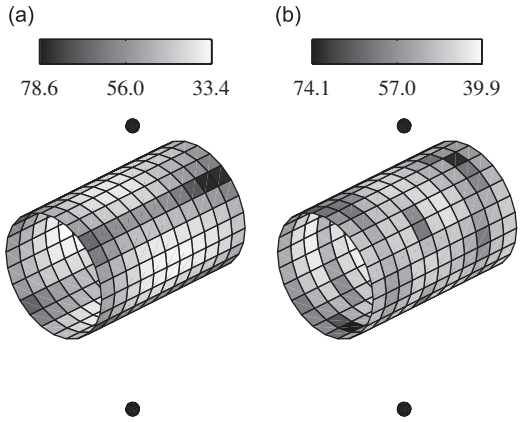

Fig. 7. The acoustic pressure amplitude on the inner surface of the cylindrical shell due to the structural vibration at (a) 100 and (b) 200 Hz. The reverse interior acoustic loading on the shell is neglected.

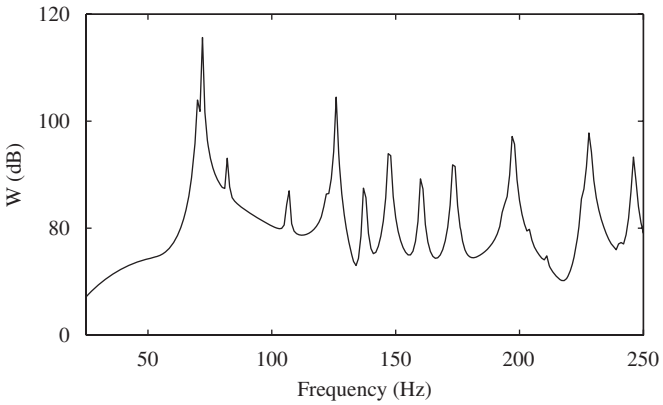

Fig. 8. The variation of the objective function as a function of frequency.

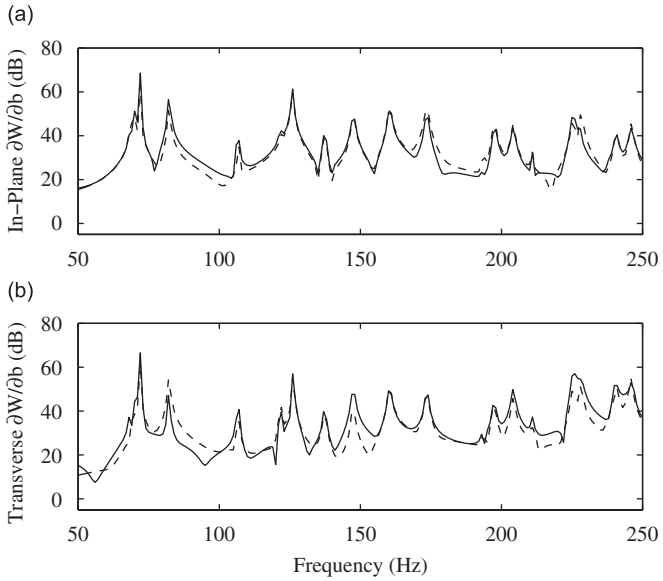

Fig. 9. The sensitivities of the objective function with respect to the in-plane reinforcement angle of the inner (solid line in (a)) and outer skin materials (dashed line in (a)), and the out-of-plane reinforcement angles in the axial direction (solid line in (b)) and in the circumferential direction (dashed line in (b)) of the core material.

where $W_{\text{ref}} = S_{\text{In}} \times 10^{-12}$ W. Examples of the sensitivity functions of the objective function with respect to the reinforcement angles of the baseline shell are shown in Fig. 9. Notice that the sensitivities of the objective function with respect to the in-plane reinforcement angles of the inner and outer skins are approximately the same. The sensitivity in dB is defined as

$$\frac{\partial W}{\partial b_i}(\text{dB}) = 10 \log_{10} |\partial W / \partial b_i|. \tag{51}$$

In the following, we present three case studies:

(1) The optimization with respect to the material reinforcement angles is studied at a single frequency 125 Hz. The initial reinforcement angles are all set to be 0°. Each angle is allowed to change between 0° and 90°. The fundamental frequency 68.70 Hz of the baseline structure is taken to be the constraint of the

Table 2
The optimal reinforcement angles from the tonal optimization

Optimal orientation angle	θ_i	θ_o	α_c	β_c
Degree	68.76	50.83	59.36	0.38

The subscripts i, o and c refer to the inner, and outer surfaces, and the core of the sandwich shell.

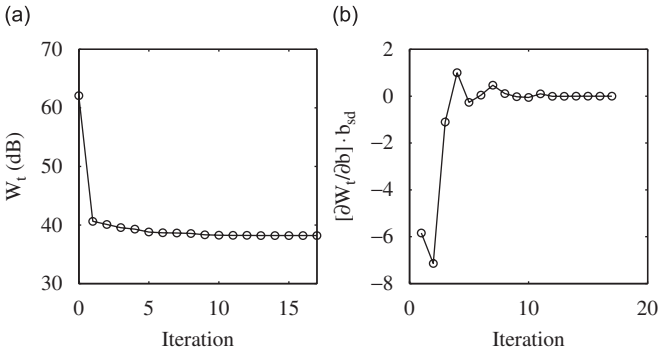

Fig. 10. (a) The history of the objective function and (b) the gradient of the objective function in the search direction for the tonal optimization at 125 Hz.

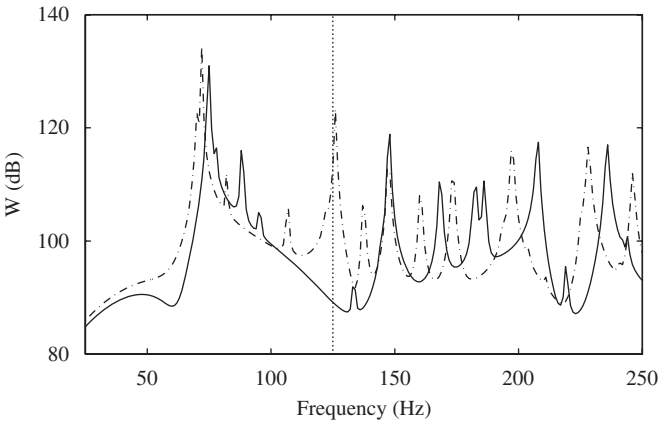

Fig. 11. The variations of the objective functions with frequency for the optimized structure at 125 Hz (solid line) and for the baseline structure (dotted–dash line).

minimum fundamental frequency. The optimal design parameters are found and listed in Table 2. The fundamental frequency of the optimized shell is 74.72 Hz.

Fig. 10 shows the history of the objective function and the sensitivity of the objective function during the optimization. The optimization has converged after 17 iterations when the sensitivity approaches zero. The objective function is reduced by 23.91 dB at 125 Hz. The objective function W in the frequency domain is shown in Fig. 11, which clearly indicates the reduction of W near 125 Hz.

(2) The optimization in a band of frequencies from 100 to 150 Hz is considered next. The design parameter bounds and fundamental frequency constraint same as in the previous case are applied. The optimal design parameters are obtained and listed in Table 3.

Table 3
The optimal reinforcement angles from the wideband optimization

Optimal orientation angle	θ_i	θ_o	α_c	β_c
Degree	87.29	50.33	58.99	0.10

The subscripts i, o and c refer to the inner and outer surfaces, and the core of the sandwich shell.

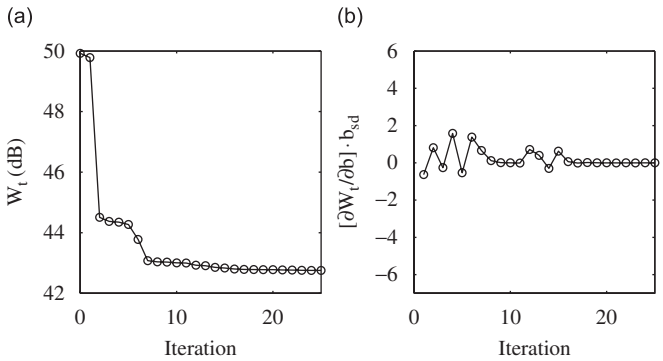

Fig. 12. (a) The history of the objective function and (b) the gradient of the objective function in the search direction for the wideband optimization (100–150 Hz).

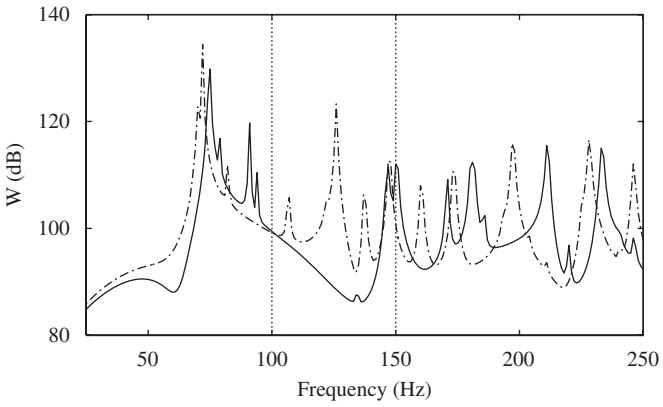

Fig. 13. The variations of the objective functions with frequency for the optimized structure in the frequency band (100–150 Hz) (solid line) and for the baseline shell (dotted–dash line).

Fig. 12 shows the history of the objective function and the sensitivity of the objective function during the optimization. We yield 7.17 dB average reduction of the transmitted acoustic power over the frequency band. The frequency variation of the objective function W is shown in Fig. 13.

(3) Here, we consider another frequency band from 150 to 200 Hz. In this case, the optimization reduces the objective function W by 3.06 dB on average over the band. The fundamental frequency of the optimized structure is 69.08 Hz. The iteration history of the optimization is shown in Fig. 14. The optimized objective function W is plotted in Fig. 15 and is compared to the baseline value in the frequency domain. (Table 4)

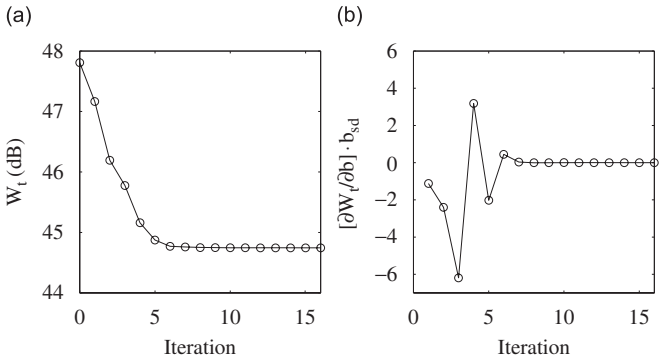

Fig. 14. (a) The history of the objective function and (b) the gradient of the objective function in the search direction for the wideband optimization (150–200 Hz).

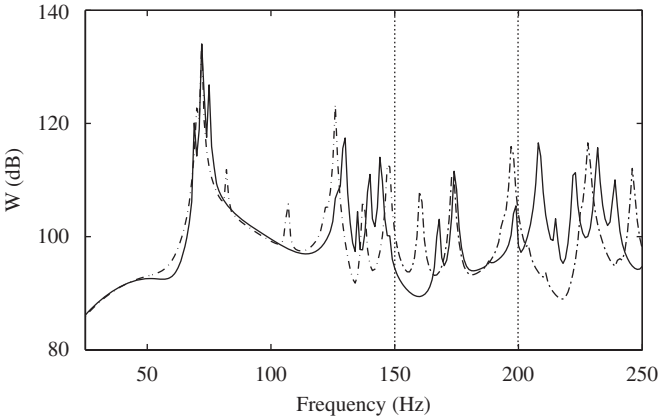

Fig. 15. The variations of the objective functions with frequency for the optimized structure in the frequency band (150–200 Hz) (solid line) and for the baseline shell (dotted–dash line).

Table 4
The optimal reinforcement angles from the wideband optimization

Optimal orientation angle	θ_i	θ_o	α_c	β_c
Degree	45.47	0.00	0.00	20.22

The subscripts i, o and c refer to the inner and outer surfaces, and the core of the sandwich shell.

7.1. Discussions

Recall that the optimization parameters are the fiber reinforcement angles of the composites in the three layers of the sandwich. Reinforcement angles can be readily achieved in the composite manufacturing process. As is the case in most structural and topological optimization studies, we do not have experimental verification of the optimum structures. The optimization results presented herein, however, do offer a general guideline on how to choose the orientation of the composite layers of the sandwich structure when the minimum sound transmission is an objective, and what one could expect when only the fiber reinforcement angles are at one's disposal. By comparing the results in the three cases, one can see that the current set of optimization parameters can provide significant tonal sound reductions, and becomes less effective in higher frequency bands. This is physically reasonable. At higher frequencies, structural damping becomes more effective in reducing vibration and sound transmission and the structural–acoustic optimization should then consider damping parameters.

The optimization solution process is computationally intensive. Most of the computational cost is for the solution of the eigen problem at every iteration. The computational time for a complete optimization solution varies significantly because the termination of the search algorithm depends on initial conditions and the optimum criteria. Each iteration of the optimizations reported above is about 40 s including sensitivity calculations. The computation was done on a PC with a dual-core 1.3 GHz Intel processor running Windows XP.

8. Concluding remarks

We have presented an optimization study of cylindrical sandwich shells to minimize the transmitted sound induced by the exterior acoustic excitations. The boundary element method is used to model the interior and exterior acoustics, and the finite elements are used to model the vibration of the shell. The design parameters of the optimization problem are the reinforcement angles of the orthotropic composite materials of the skins and core. The sensitivity of the objective function with respect to the design variables has been analyzed, and the adjoint variable method is adopted for the solution of sensitivity functions. The optimizations of the shell at a single frequency and in a band of frequencies are investigated. The results of optimization show that it is possible to optimally design composite sandwich shells to minimize the sound transmission into the interior at low frequencies. At higher frequencies where structural damping is more effective in reducing vibration and sound transmission, the fiber reinforcement angles are no longer sufficient to reduce sound transmission significantly.

Acknowledgment

This paper is based on the work supported by a grant (CMS-0219217) from the National Science Foundation.

References

[1] L.A. Krakers, M.J.L.V. Tooren, K. Zaal, C.A.J.R. Vermeeren, Integration of acoustics and mechanics in a stiffened shell fuselage. Part III, *Applied Composite Materials* 12 (1) (2005) 21–35.

[2] M.J.L.V. Tooren, L.A. Krakers, A. Beukers, Integration of mechanics and acoustics in a sandwich fuselage. Part IV, *Applied Composite Materials* 12 (1) (2005) 37–51.

[3] P. Thamburaj, Structural–acoustic Studies of Sandwich Structures for Global Transport Aircraft, PhD Thesis, University of Delaware, 2001.

[4] P. Thamburaj, J.Q. Sun, Optimization of anisotropic sandwich beams for higher sound transmission loss, *Journal of Sound and Vibration* 254 (1) (2002) 23–36.

[5] F. Franco, K.A. Cunefare, M. Ruzzene, Structural–acoustic optimization of sandwich panels, Proceedings of the ASME International Design Engineering Technical Conferences and Computers and Information in Engineering Conference (DETC2005), Vol. 1 C, Long Beach, California, September 2005, pp. 2391–2400.

[6] E.W. Constans, G.H. Koopmann, A.D. Belegundu, Use of modal tailoring to minimize the radiated sound power of vibrating shells: theory and experiment, *Journal of Sound and Vibration* 217 (2) (1998) 335–350.
[7] W.M. Johnson, K.A. Cunefare, Structural acoustic optimization of a composite cylindrical shell using FEM/BEM, *Journal of Vibration and Acoustics* 124 (3) (2002) 410–413.
[8] F. Fahy, *Sound Structural Vibration: Radiation Transmission and Response*, Academic Press, Inc., Orlando, FL, 1985.
[9] M.D. Greenberg, *Advanced Engineering Mathematics*, Prentice-Hall, Inc., Upper Saddle River, NJ, 1998.
[10] T.W. Wu, *Boundary Element Acoustics: Fundamentals and Computer Codes*, Wit Press, Boston, MA, 2000.
[11] T.W. Chou, *Microstructural Design of Fiber Composites*, Cambridge University Press, Cambridge, UK, 1992.
[12] J.R. Vinson, *The Behavior of Sandwich Structures of Isotropic and Composite Materials*, Technomic Publishing Company, Lancaster, PA, 1999.
[13] D.P. Bertsekas, *Constrained Optimization and Lagrange Multiplier Methods*, Academic Press, New York, 1982.
[14] R.R. Salagame, A.D. Belegundu, G.H. Koopmann, Analytical sensitivity of acoustic power radiated from plates, *Journal of Vibration and Acoustics* 117 (1) (1995) 13–18.
[15] Y.W. Kwon, H. Bang, *The Finite Element Method Using Matlab*, CRC Press, Boca Raton, FL, 2000.